Current Applied Physics 9 (2009) 1097–1105

Contents lists available at ScienceDirect

Current Applied Physics

journal homepage: www.elsevier.com/locate/cap

Effect of Ag doping on the crystallization and phase transition of TiO_2 nanoparticles

J. García-Serrano [a], E. Gómez-Hernández [b], M. Ocampo-Fernández [c], U. Pal [c,*]

[a] Centro de Investigaciones en Materiales y Metalurgia, Universidad Autónoma del Estado de Hidalgo, Carretera Pachuca Tulancingo Km 4.5, Mineral de la Reforma, Hidalgo, C.P. 42184, Mexico
[b] Universidad Popular Autónoma del Estado de Puebla, 21 sur 1103, Col. Santiago, C.P. 72410, Puebla, Pue., Mexico
[c] Instituto de Física, Universidad Autónoma de Puebla, Apdo. Postal J-48, Puebla, Pue. 72570, Mexico

ARTICLE INFO

Article history:
Received 21 October 2008
Received in revised form 22 November 2008
Accepted 18 December 2008
Available online 31 December 2008

PACS:
61.46.Hk
61.46.−w
64.70.Nd
81.07.−b

Keywords:
TiO_2 nanoparticles
Doping
Crystallization
Phase transition

ABSTRACT

TiO_2 nanoparticles doped with different Ag contents were prepared by a modified sol–gel method, using titanium tetraisopropoxide and silver nitrate as precursors and 2-propanol as solvent. Silver was incorporated into the TiO_2 matrix via decomposition of $AgNO_3$ during thermal treatment in different atmospheres. Effects of Ag doping on the crystallization and phase transition of the TiO_2 nanoparticles were studied using differential scanning calorimetry (DSC), thermogravimetric analysis (TGA), X-ray diffraction (XRD), and Raman spectroscopy techniques. While air annealing incorporates silver into TiO_2 matrix in silver oxide form, annealing in nitrogen incorporates metallic silver into TiO_2. Formation of silver oxide increases the thermal stability of the TiO_2 particles. Silver oxide affects the crystallization process of TiO_2 particles and the temperature of transition form anatase to rutile. On the other hand, presence of metallic silver in the samples annealed in nitrogen atmosphere decreases the temperature of phase transition of TiO_2 nanoparticles.

1. Introduction

In recent years, the preparation and characterization of titanium oxide (TiO_2) nanostructures have attracted much interest due to their unique properties and potential applications in catalysis [1–3], photo-catalysis [4–9], sensors [10,11], solar cells [12–14], energy storage [15], and gene therapy [16,17], among others. It has been demonstrated that the physical and chemical properties of TiO_2 nanostructures, and hence their potential applications depend strongly on their crystalline structure, morphology and particle size [18]. TiO_2 occurs mainly in three crystalline phases namely anatase, rutile and brookite; and rutile is the thermodynamically most stable phase. They differ in their physical properties, such as refractive index, dielectric constant, chemical and photochemical reactivity. It is well known that the photocatalytic activity of TiO_2 is intimately related with its crystal structure [19]. While TiO_2 in anatase phase has high photocatalytic activity, the rutile TiO_2 shows no appreciable activity. Also, the surface area, particle size, surface hydroxyl groups, film thickness, and UV light intensity have been seen to be the additional parameters influencing the photocatalytic activity of crystalline TiO_2 [20–22]. On the other hand, the modification of TiO_2 by means of metal doping can also affect the crystallization process, influencing the photocatalytic efficiency of TiO_2. Recently, Tomaszewski et al. [23] have reported that a reduced sodium concentration in TiO_2 films leads to well crystallized anatase phase after annealing, and increases their photocatalytic activity. Several works have been published on the incorporation of small metal particles, in particular noble metal particles (Ag, Au and Pt) for improving the photocatalytic and photo-electrochemical activities of TiO_2 [24–26]. Addition of small amounts of metal can induce crystallization in amorphous materials on annealing at relatively low temperatures. This process, known as metal-induced crystallization, has been applied by Izmajlowicz et al. [27] for significant reduction of the solid-phase crystallization temperature of amorphous silicon. Crystallization process induced by Au nanoparticles has been studied in thin films of ceramic materials such as SiO_2, TiO_2, and ZrO_2 [28]. Very recently Perkas et al. [29] have reported that insertion of Au nanoparticles into titania by sonochemical reduction of gold ions in ethylene glycol at 80 °C yields anatase phase. There exist many contradictory reports on the crystallization and phase transformation of TiO_2 [30–33]. Though crystallization and phase transformation are essential for many applications involving TiO_2 nanoparticles, it is evident that these can be influenced by the synthesis process, starting materials, and impurities or doping species.

* Corresponding author. Tel.: +52 222 2295500; fax: +52 222 2295611.
E-mail address: upal@sirio.ifuap.buap.mx (U. Pal).

1567-1739/$ - see front matter © 2008 Elsevier B.V. All rights reserved.
doi:10.1016/j.cap.2008.12.008

In the present work, we report on the synthesis of TiO_2 and Ag doped TiO_2 nanoparticles through a modified sol–gel method, using titanium tetraisopropoxide and silver nitrate as precursors and 2-propanol as solvent. The silver was incorporated into the TiO_2 matrix during the thermal treatment of the gel material in air or N_2 via decomposition of $AgNO_3$. The effects of Ag doping on the morphology, crystallization and phase transition of TiO_2 nanoparticles are studied by X-ray diffraction (XRD), scanning electron microscopy (SEM), Raman and FT-IR spectroscopy, thermogravimetric analysis (TGA), and differential scanning calorimetry (DSC) techniques. In general, Ag doping increases the thermal stability of the TiO_2 particles when the annealing is performed in air. While Ag doping affects the crystallization process of TiO_2 particles, concentration of metallic silver, silver oxide doping and the nature of annealing atmosphere control the temperature of phase transition from anatase to rutile.

2. Experimental section

2.1. Materials

Titanium tetraisopropoxide (Ti [OCH $(CH_3)_2]_4$, TTP, 97%) and silver nitrate ($AgNO_3$, 99.99%) were purchased from Aldrich. 2-propanol ($CH_3CHOHCH_3$, 2P, 99.8%) was purchased from J.T. Baker. All the materials were used as received.

2.2. Preparation of TiO_2 support

For the preparation of support solution used for the synthesis of TiO_2 and Ag doped TiO_2 particles, 14.6 ml of TTP was added dropwise to 248.8 ml of 2-propanol under vigorous stirring at room temperature in a glove box under nitrogen atmosphere. The resultant mixture was magnetically stirred for 1 h at room temperature and then kept in the glove box without agitation for 24 h.

2.3. Preparation of TiO_2 nanoparticles

TiO_2 nanoparticles were synthesized through a modified sol–gel method. First, 131.73 ml of support (TTP–2P) solution was hydrolyzed by 9.01 ml of water, which was added drop wise under vigorous stirring. The resulting sol was stirred for 1 h and maintained in the glove box for 24 h. Then, the formed gel was dried for 12 h at 100 °C in air. The obtained powder sample was heated for 4 h in air or under N_2 atmosphere at different temperatures (300, 450, 600, 700 and 750 °C), with a heating rate of 240 °C/h.

2.4. Preparation of Ag doped TiO_2 particles

The synthesis procedure for Ag–TiO_2 nanocomposites was analogous to the one used for TiO_2 nanoparticles. However, for Ag doping, different amounts of $AgNO_3$ (0.1698, 0.2831 and 0.4247 g) were added to the reaction mixture. In a typical synthesis process, 131.73 ml of the support solution (TTP–2P) was hydrolyzed by slow addition of a solution containing the desired amount of $AgNO_3$ dissolved in 9.01 ml of water. After that, the resulting mixture was maintained in the glove box for 24 h, obtaining a dark yellow gel. The gels prepared with different $AgNO_3$ contents were dried for 12 h at 100 °C in air, and then treated thermally for 4 h under air under N_2 atmosphere at 300, 450, 600, 700 and 750 °C, with a heating rate of 240 °C/h.

2.5. Characterizations

X-ray diffraction measurements on the samples were performed in a Phillips X'Pert diffractometer in the 20–80° range using Cu Kα (λ = 1.5406 Å) radiation. Scanning electron microscopic (SEM) images were recorded with a JEOL JSM LV-5600 microscope. A Nicolet Magna 750 FT-IR spectrometer was used to record the IR absorption spectra of the samples in the 4000–400 cm^{-1} spectral range. For FT-IR studies, 1 mg of solid sample was mixed with 99 mg of dry KBr homogeneously to make pellets of 7 mm diameter and 0.5 mm thick. A Perkin–Elmer NIR Spectrum GX FT-Raman spectrometer with Nd:YAG laser source was used for recording Raman spectra of the samples at room temperature. Thermogravimetric measurements were carried out with a Mettler-Toledo TGA/SDTA 851 thermal gravimetric analyzer. The measurements were performed from room temperature to 1000 °C, at a heating rate of 10 °C/min under nitrogen atmosphere. Differential scanning calorimetry measurements were carried out with a Mettler-Toledo DSC-822e calorimeter. The measurements were performed from room temperature to 750 °C, at a heating rate of 10 °C/min under nitrogen atmosphere.

3. Results and discussion

Fig. 1 shows the XRD patterns of the undoped TiO_2 powders after annealing at different temperatures in air for 4 h. The as-prepared TiO_2 powders were found to be amorphous. The XRD pattern of the TiO_2 sample annealed at 450 °C revealed 12 peaks in the range of $2\theta = 25.0 - 76.0°$, assigned as (101), (103), (004), (112), (200), (105), (211), (204), (116), (220), (215), and (301) reflections corresponding to the anatase phase. This indicates that the amorphous TiO_2 nanoparticles crystallized in anatase phase at a temperature below 450 °C. The XRD pattern of the TiO_2 sample annealed at 600 °C revealed few rutile peaks in addition to the peaks corresponding to anatase phase, which indicates that the phase transformation from anatase to rutile starts in the temperature range 450–600 °C. Through semi-quantitative XRD analysis, the fractions of the anatase and rutile phases in this sample were estimated to be about 47.83% and 52.17%, respectively. For annealing above 600 °C, the relative intensity of the anatase peaks with respect to rutile peaks decreased and finally vanished. In the XRD pattern of the TiO_2 sample annealed at 750 °C, practically only the peaks assigned to the rutile phase were observed, indicating a complete phase transformation from anatase to rutile at this temperature.

Fig. 2 shows the XRD patterns of the undoped TiO_2 powders annealed at different temperatures under N_2 atmosphere. The as-prepared TiO_2 powders were found to be amorphous as discussed earlier. The XRD pattern of the TiO_2 sample annealed at 450 °C revealed 12 peaks in the range of $2\theta = 25.0 - 76.0°$, assigned as (101), (103), (004), (112), (200), (105), (211), (204), (116), (220), (215), and (301) reflections corresponding to the anatase phase, along with 10 peaks assigned as (110), (101), (111), (210), (211), (220), (002), (310), (301), and (112) reflections in the same range corresponding to the rutile phase. This shows that the amorphous TiO_2 nanoparticles crystallized in the anatase and rutile phase at a temperature below 450 °C while annealing under N_2 atmosphere. In the XRD pattern of the TiO_2 sample annealed at 700 °C, the relative intensity of the anatase peaks with respect to rutile peaks decreased significantly but never disappeared. The XRD pattern also revealed three more peaks assigned as (002), (301), (202) reflections of the rutile phase, indicating an incomplete phase transformation from anatase to rutile at this temperature.

XRD patterns of the Ag–TiO_2 composites synthesized with different $AgNO_3$ contents before and after annealing in air at different temperatures are shown in the Fig. 3. From the diffraction patterns, we can observe: (i) all the as-prepared Ag–TiO_2 composites are amorphous; (ii) Ag–TiO_2 composites annealed at 450 °C reveal sev-

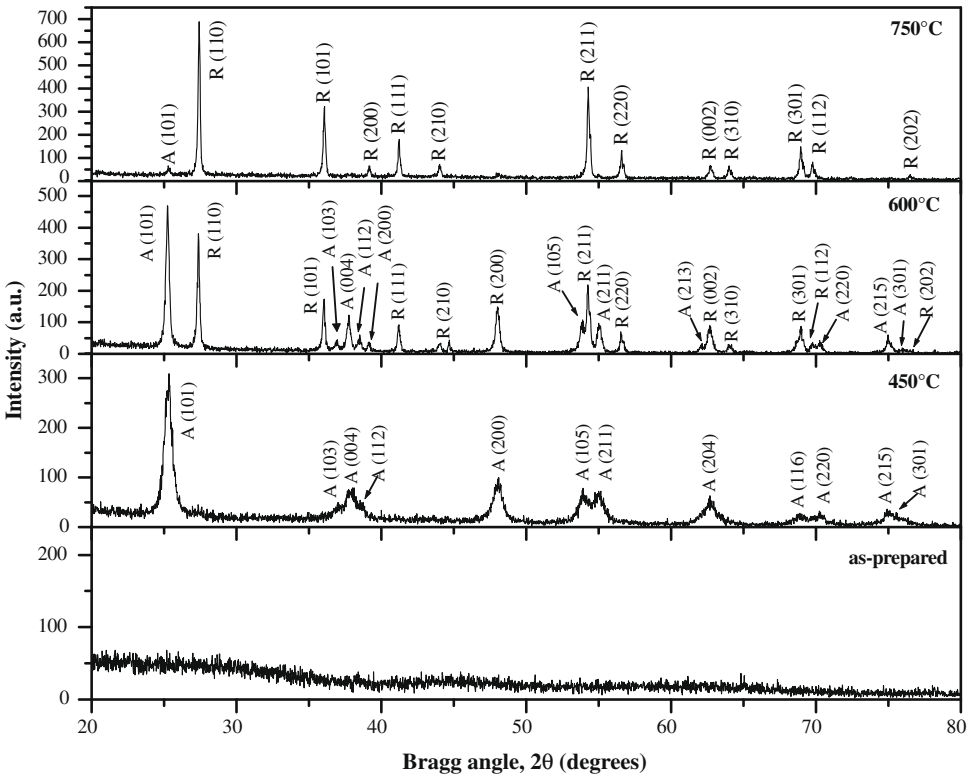

Fig. 1. X-ray diffraction patterns of the TiO_2 powders before and after annealing at different temperatures in air for 4 h. A and R represents anatase and rutile phases, respectively.

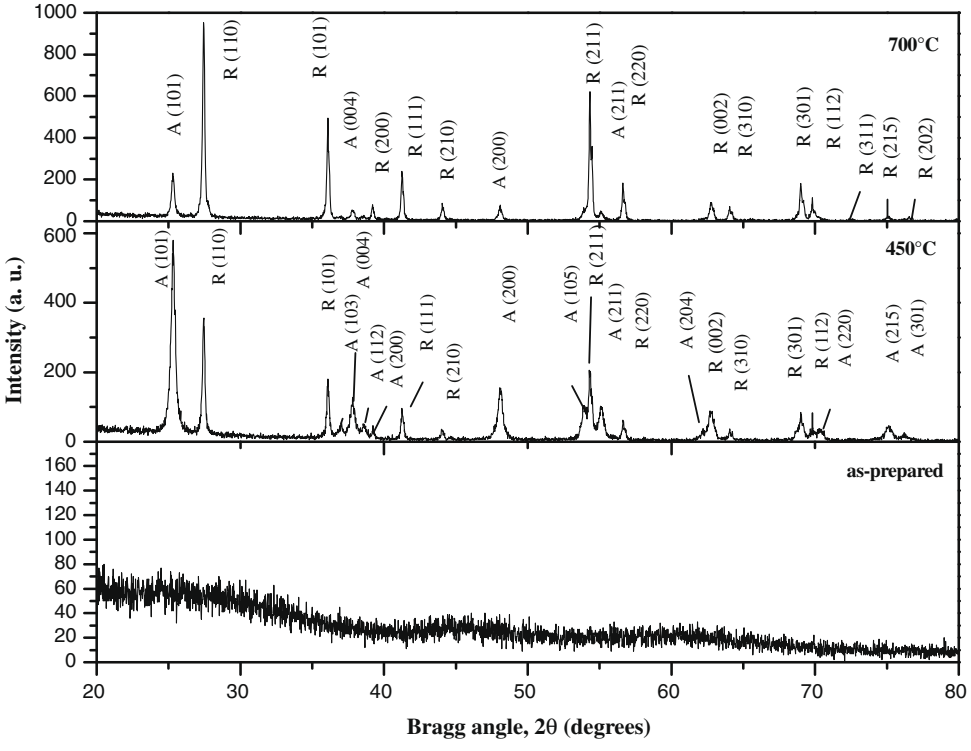

Fig. 2. X-ray diffraction patterns of the TiO_2 powders before and after annealing at different temperatures in N_2 for 4 h. A and R represents anatase and rutile phases, respectively.

eral diffraction peaks associated to the anatase TiO_2 and crystalline silver oxide compounds, along with some diffraction peaks corresponding to metallic silver in face centered cubic phase for high $AgNO_3$ contents (0.2831 and 0.4247 g of $AgNO_3$). Therefore, the amorphous TiO_2 crystallizes in the anatase phase at a temperature below 450 °C and the incorporated Ag in the TiO_2 matrix remains

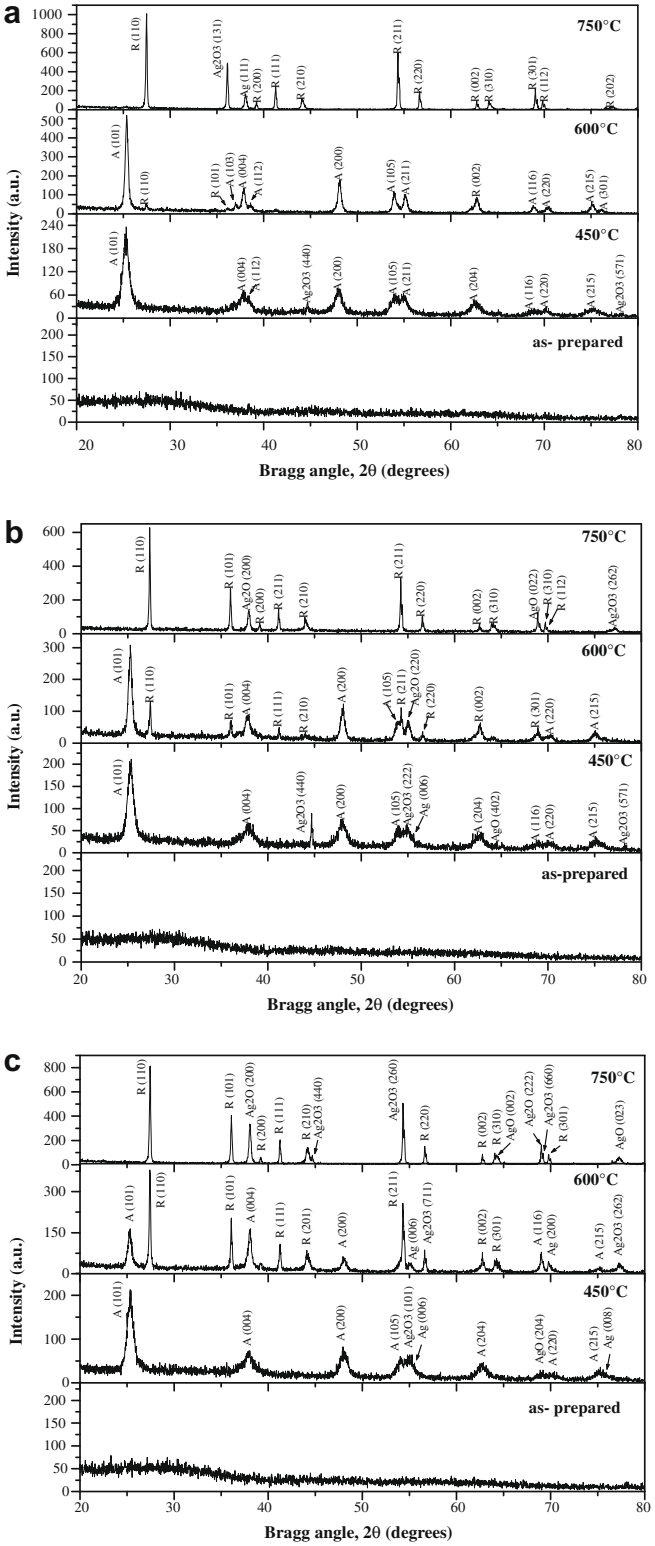

Fig. 3. X-ray diffraction patterns of the Ag–TiO_2 composites synthesized using (a) 0.1698 g, (b) 0.2831 g, and (c) 0.4247 g of $AgNO_3$, before and after annealing at different temperatures in air for 4 h. A and R represents anatase and rutile phases, respectively.

mainly in oxide forms. (iii) On increasing the annealing temperature to 600 °C, the relative intensity of the anatase peaks decreases, and the peaks related to the rutile phase emerges. The intensity of the rutile peaks increased with the increase of Ag content in the composites. Volume fraction of the rutile phase increased from 52.17% to 56.25% on incorporating Ag in the TiO_2 particles (0.4247 g of $AgNO_3$) during synthesis. This indicates that the presence of Ag species enhances the phase transformation (anatase to rutile) process in TiO_2. (iv) On annealing at 750 °C, only the peaks correspond to the rutile and crystalline silver oxide species were observed. Absence of any peak characteristic of anatase phase in the sample suggests that the transformation from anatase to rutile finishes well below 750 °C while annealing in air atmosphere, due to the presence of the silver oxide species.

XRD patterns of the Ag–TiO_2 composites synthesized with different $AgNO_3$ contents with and without annealing treatments at different temperatures in N_2 atmosphere are shown in Fig. 4. From the diffraction patterns we can observe: (i) all the as-prepared Ag–TiO_2 composites are amorphous; (ii) Ag–TiO_2 composites annealed at 300 °C reveals six diffraction peaks associated to the anatase TiO_2, while metallic silver is not yet formed. Therefore, the amorphous TiO_2 crystallizes in the anatase phase at a temperature below 300 °C in N_2 atmosphere. (iii) On increasing the annealing temperature to 450 °C, the relative intensity of the anatase peaks increased, the peaks related to the rutile phase did not emerge, and only a small peak corresponding to metallic Ag evolved. (iv) On annealing at 700 °C, the peaks corresponding to anatase, rutile and crystalline Ag species evolved. The low intensity of the rutile peaks suggests that the transformation from anatase to rutile was retarded due to the presence silver while annealing in N_2 atmosphere.

Figs. 5 and 6 show the typical SEM images of TiO_2 samples synthesized with and without Ag doping. SEM image (Fig. 5a) of the as-prepared TiO_2 shows irregular porous particles of ~140 nm average size, formed by the aggregation of small spherical particles of dispersed sizes. Annealing of the TiO_2 sample at 750 °C produced more homogeneous spherical particles, which aggregated to form bigger particles with porous structures (Fig. 5b). Similar morphology is obtained for the Ag–TiO_2 composites annealed at 750 °C (Fig. 6b), whereas the morphology of the as-prepared Ag–TiO_2 composites is significantly different (Fig 6a). As-grown Ag–TiO_2 composites revealed relatively compact surface morphology with low porosity in comparison with the undoped as-prepared TiO_2 samples (Fig. 5a). In general, the average particle size decreased on incorporation of Ag in TiO_2.

Annealing induced phase transition in TiO_2 particles was further monitored by Raman spectroscopy. In the Fig. 7, Raman spectra of the undoped TiO_2 samples annealed at different temperatures in air are presented. While the as-prepared sample showed spectral features basically corresponding to the amorphous phase, the sample annealed at 450 °C revealed several bands at about 206, 396, 517, 637, and 669 cm^{-1}. These bands are the characteristic E_g (low-frequency), B_{1g}, A_{1g}, E_g (high-frequency), and B_{1g} vibrational modes of anatase phase [34,35], respectively. With the increase of annealing temperature to 600 °C, the intensity of these anatase bands increased while two new bands at about 447 and 609 cm^{-1}, which correspond to the characteristic E_g and A_{1g} vibrational modes of rutile phase, respectively, appeared [36]. For the TiO_2 sample annealed at 750 °C, the intensity of the rutile bands became stronger while the anatase bands disappeared, indicating a complete phase transition from anatase to rutile. Phase transitions observed in the Raman spectra are in complete agreement with our XRD results.

Fig. 8 shows the FT-IR spectra of the TiO_2 particles before and after annealing at 450 °C, along with of as-prepared Ag–TiO_2 samples. For the as-prepared TiO_2 sample (Fig. 8a) several absorption bands correspond to the vibrational modes of organic species such as hydroxyl, carboxilate and alkane groups are observed. A broad band observed in between 3700 and 3000 cm^{-1} is related to the O–H stretching mode of hydroxyl group, indicating the presence

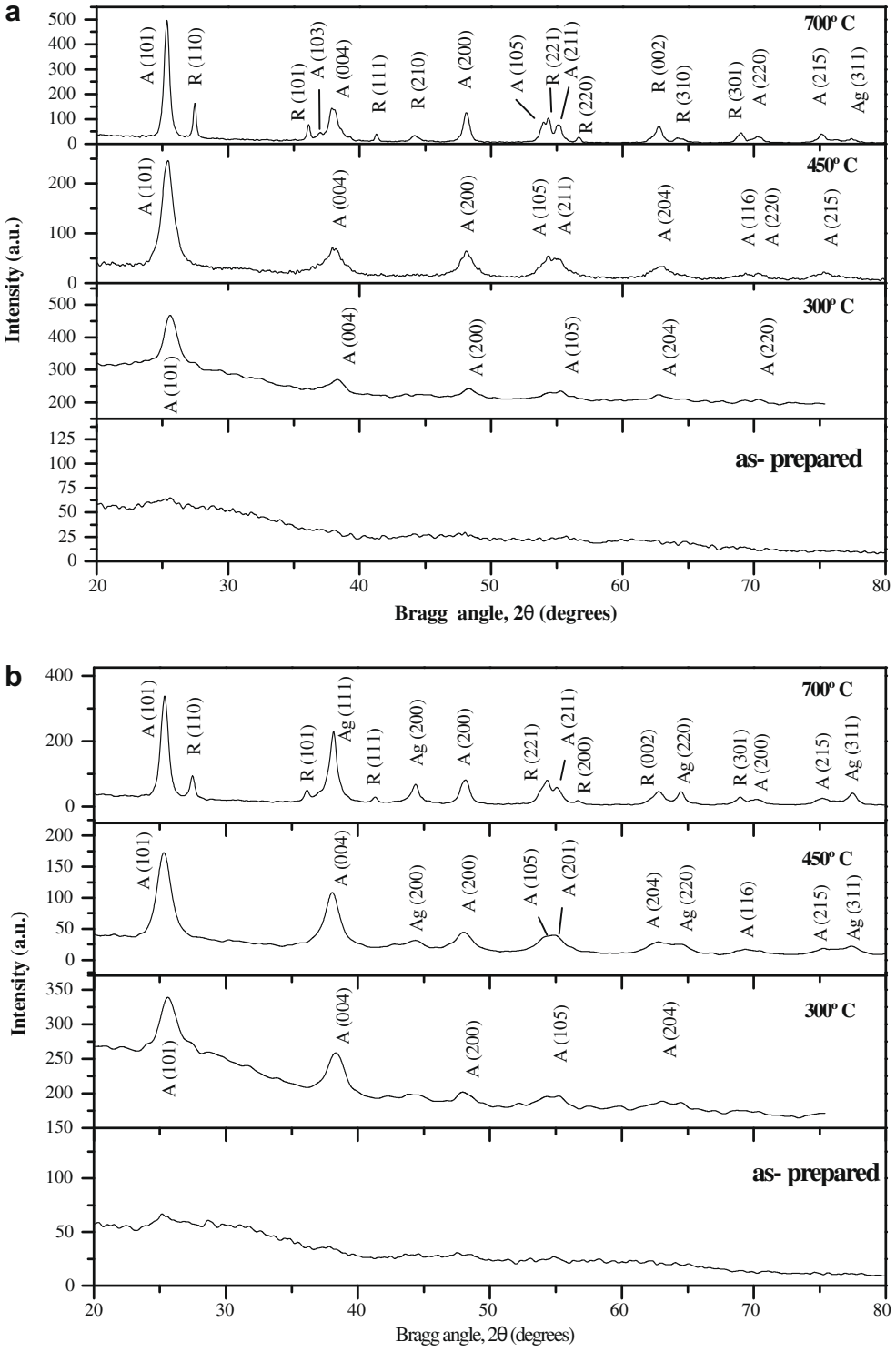

Fig. 4. X-ray diffraction patterns of the Ag–TiO_2 composites synthesized using (a) 0.1698 g, and (b) 0.4247 g of $AgNO_3$, before and after annealing at different temperatures in N_2 for 4 h. A and R represents anatase and rutile phases, respectively.

of moisture in the sample. The peaks in between 3000 and 2800 cm^{-1} are assigned to C–H stretching vibrations of alkane groups. The peak at 1636 cm^{-1} can be associated to the asymmetric stretching mode of titanium carboxilate. The alkane and carboxilate groups come from TTP and 2-propanol precursors used in the synthesis process. The strong absorption band observed in between 800 and 450 cm^{-1} can bee associated to the vibrational modes of TiO_2. On annealing at 450 °C the intensity of the bands associated with the organic groups decreased significantly (Fig. 8b), indicating the elimination of organic species in the sample. On the other hand, all the IR spectra of Ag–TiO_2 samples revealed a peak at about 1385 cm^{-1}, which was not observed for the undoped TiO_2. The intensity of this peak increased with the increase of silver precursor ($AgNO_3$) in the composite samples. The peak at 1385 cm^{-1} was assigned tentatively to the interaction between Ag and TiO_2 particles.

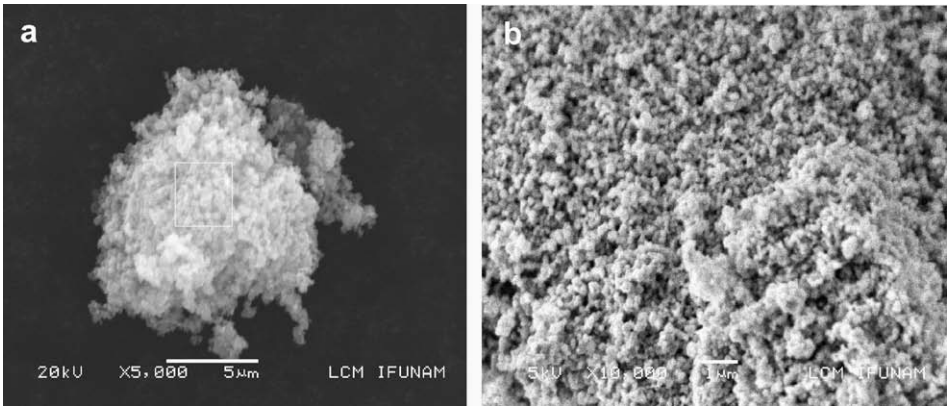

Fig. 5. Typical SEM images of the (a) as-prepared and (b) 750 °C annealed undoped TiO_2 samples.

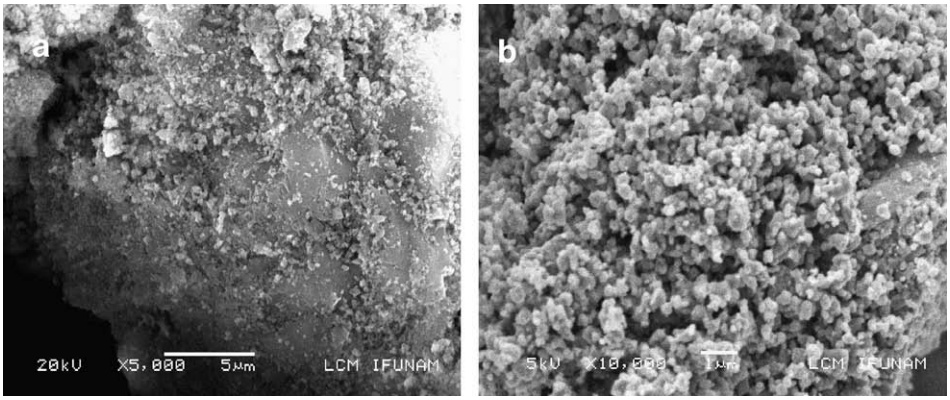

Fig. 6. Typical SEM images of the (a) as- prepared Ag–TiO_2 composite synthesized using 0.2831 g of $AgNO_3$, and (b) Ag–TiO_2 composite synthesized using 0.1698 g of $AgNO_3$ after annealing at 750 °C.

The thermal evolution of the TiO_2 and Ag–TiO_2 samples under nitrogen atmosphere was studied using thermogravimetric analysis (TGA) and differential scanning calorimetry (DSC) techniques. Fig. 9 shows typical TGA thermograms of the Ag–TiO_2 composite synthesized using 0.2831 g of $AgNO_3$ and annealed at different temperatures in air. Analysis of the TGA thermograms of the as-prepared sample revealed three distinct regions of weight loss. The first region, a gradual weight loss of about 15% beginning at 25 °C and ending at 235 °C, was associated to the loss of residual water and 2-propanol in the samples. This indicates that although the samples were dried for 12 h at 100 °C in air, water and 2-pro-

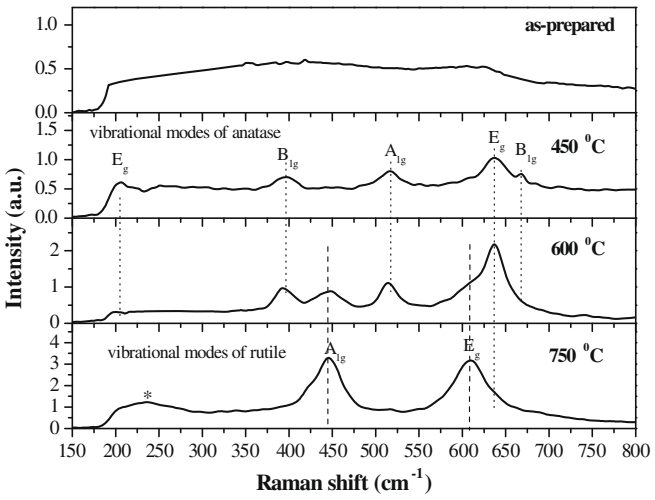

Fig. 7. Raman spectra of the undoped TiO_2 particles annealed at different temperatures in air.

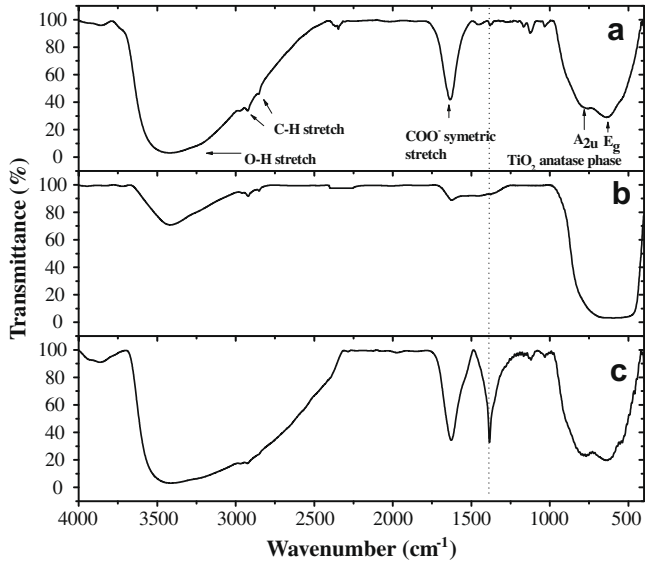

Fig. 8. FT-IR spectra of the (a) as-prepared TiO_2, (b) TiO_2 annealed at 450 °C in air, and (c) as-prepared Ag–TiO_2 composites.

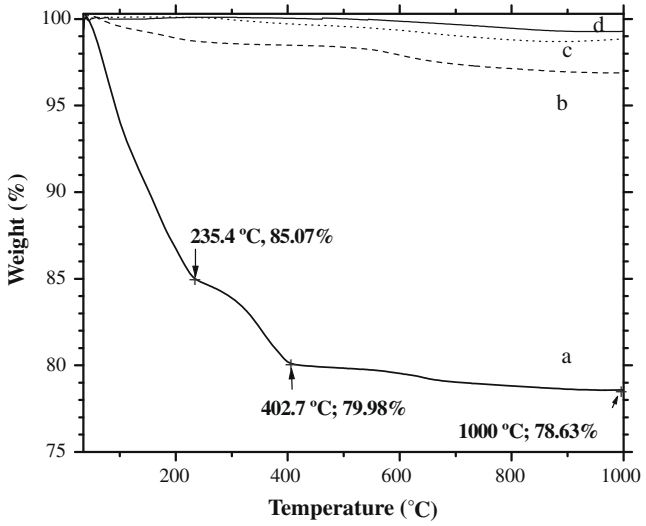

Fig. 9. TGA thermograms of the Ag–TiO_2 composites synthesized using 0.2831 g of $AgNO_3$; (a) as-prepared, annealed at: (b) 450 °C, (c) 600 °C, and (d) 750 °C in air.

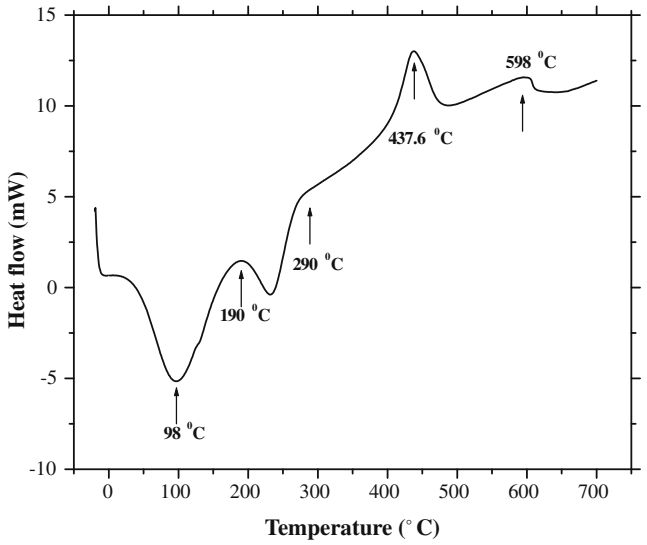

Fig. 10. DSC curve of as-prepared TiO_2 particles. The measurement was performed from room temperature to 750 °C, at a heating rate of 10 °C/min under nitrogen atmosphere.

panol were not eliminated completely until about 235 °C temperature. In the second region, about 5% of weight was lost between 230 and 403 °C. Such weight loss can be associated to the elimination of organic components. Finally, the last weight loss occurred above 403 °C, which represents approximately 1% of initial solid weight.

On the other hand, as expected for the Ag–TiO_2 composite samples annealed at 450 °C or higher, the weight losses associated to the elimination of water and organic components decreased or absent in their TGA thermograms. The TGA curves of the Ag–TiO_2 composites annealed at 450, 600, and 750 °C revealed only one weight loss throughout the whole measurement range, representing approximately 3%, 1.2%, and 0.7% of the initial weight, respectively, indicating the elimination of practically all water and organic species by the thermal treatments before realizing the TGA analysis. The results are in well agreement with the IR analysis presented earlier. The TGA thermograms of Ag–TiO_2 composites synthesized with 0.1698 g and 0.4247 g of $AgNO_3$ revealed similar characteristics as that of Ag–TiO_2 composite prepared with 0.2831 g of $AgNO_3$.

DSC analysis was performed to determine the effect of silver doping on the crystallization and phase transformation behavior of the TiO_2 nanoparticles. Fig. 10 shows the DSC curve of the as-prepared TiO_2 particles. The DSC curve revealed an endothermic peak centered at about 98 °C and four exothermic peaks located at about 190, 290, 437, and 598 °C. The endothermic peak was attributed to the elimination of water adsorbed on the surface of the TiO_2 particles. The broad nature of the endothermic peak leads to the conclusion that the dehydration in TiO_2 is a slow process. On the other hand, XRD analysis has shown that the TiO_2 particles heated in air at 100 °C were amorphous in nature and after annealing at 450 °C they transform to anatase phase completely. Therefore, the first exothermic peak observed at about 190 °C can be attributed to the crystallization of amorphous TiO_2 to anatase phase, indicating that the TiO_2 nanoparticles obtained by our modified sol–gel method crystallize at relatively lower temperature. The second exothermic peak at about 290 °C was not well resolved in the DSC measurement. However, this temperature corresponds to the temperature associated to the elimination of organic components as observed in the TGA thermogram (Fig. 9). From TGA thermogram it can also be observed that the process associated with the organic species elimination is a complicated one. These results suggest that the elimination of organic compounds does not occur by means of a simple desorption process, but also involves the chemical decomposition of the species during a combustion process. Therefore, the DSC exothermic peak at 290 °C was associated to the combustion process of the organic species. On the other hand, the exothermic peak observed at about 437 °C was attributed to the phase transformation from anatase to rutile, in agreement with the previously reported results [37]. We assigned the exothermic peak at about 598 °C to the rutile phase formation. It should be remembered that the XRD and Raman results (Figs. 1 and 7) of the undoped TiO_2 particles revealed the occurrence of anatase–rutile phase transition in between 450 and 750 °C. It is important to note that while our XRD and Raman analysis revealed only the anatase phase after annealing the sample at 450 °C, the DSC curve of the sample indicates that the phase transformation starts even below 450 °C. To verify this point, we performed a DSC analysis of the sample after annealing at 450 °C. However, no peak corresponding to anatase–rutile transition was observed for the sample. This suggests in fact the anatase–rutile transition starts at temperature below 450 °C, which could not be detected from the XRD and Raman spectra of the sample.

As the nucleation and growth in solid state can occur through different rate controlled processes like diffusion and/or phase boundary reaction, a plausible explanation for the discrepancies between the XRD and DCS results can be given by considering the phase transformation process in our nanostructures. Probably, the transformation from anatase to rutile phase in our samples occurs through nucleation and growth of rutile phase in the bulk, e.g. from the center of the particles, beginning at about 437 °C. Then, the growth of rutile propagates slowly from the centre of the particles to the surface, as shown in the Fig. 11. The formation of rutile phase can be detected by XRD when it is extended near to the surface of the particles. Therefore, until a good fraction of the particles does not transform to rutile, it could not be detected in their XRD patterns.

In the Fig. 12, the DSC curves of the Ag–TiO_2 composite particles synthesized using three different amounts of $AgNO_3$ are presented. From the DSC curves, we can observe an endothermic peak at about 98 °C for all the three samples, which correspond to the dehydration process. The peak related to organic species elimination can be found at about 290 °C for all the Ag–TiO_2 samples. The fact that the peaks attributed to the dehydration process and

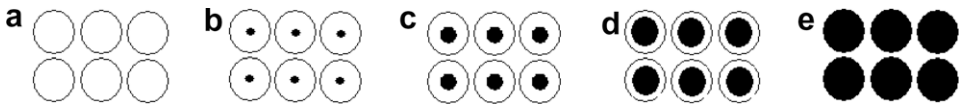

Fig. 11. Schematic presentation of the proposed phase transformation process in the sol–gel grown TiO_2 nanoparticles: (a) particles of TiO_2 crystallized with anatase phase; (b) nucleation of rutile crystals at around 437 °C; (c) growth of rutile crystals at temperatures in between 437 and 550 °C; (d) growth of rutile crystals close to the surface of the particles at 600 °C; (e) complete transformation of the crystals to the rutile phase at 750 °C.

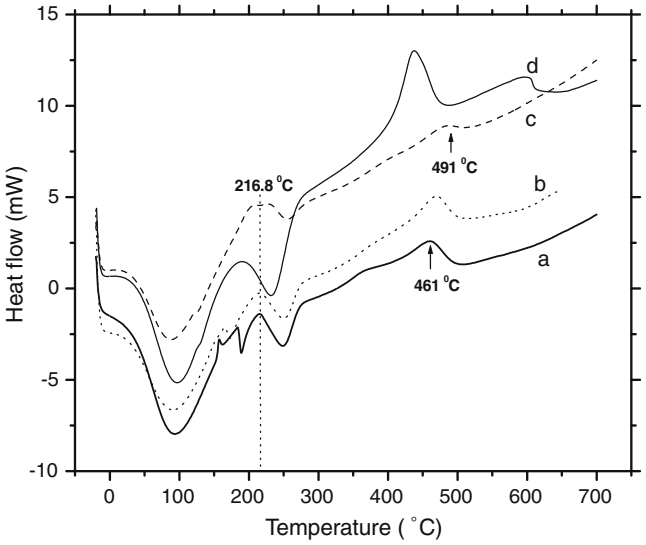

Fig. 12. DSC curves of as-prepared sol–gel grown Ag–TiO_2 composites prepared with (a) 0.1698 g, (b) 0.2831 g, and (c) 4247 g of $AgNO_3$. The measurements were performed from room temperature to 750 °C, at a heating rate of 10 °C/min under nitrogen atmosphere.

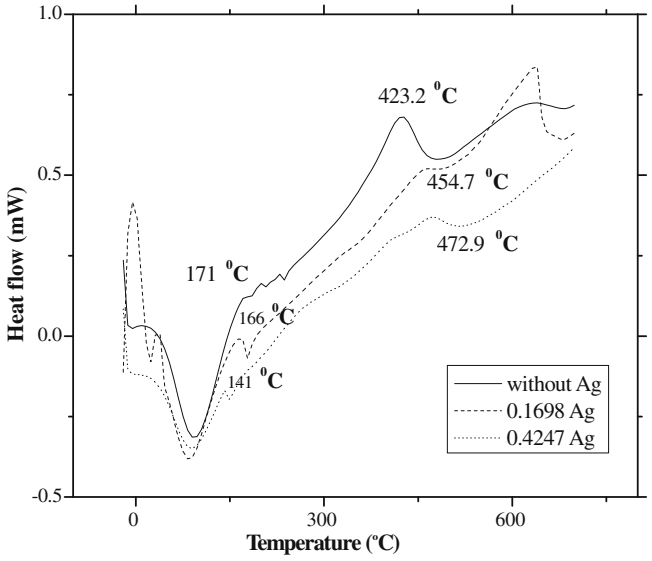

Fig. 13. DSC curves Ag–TiO_2 composites prepared without silver, with 0.1698 g and 0.4247 g of $AgNO_3$ and annealed at 300 °C in nitrogen atmosphere for 4 h. The measurements were performed from room temperature to 700 °C, at a heating rate of 10 °C/min under nitrogen atmosphere.

decomposition of organic species were observed at the same temperatures (98 and 290 °C, respectively) in both TiO_2 and Ag–TiO_2 nanoparticles indicates that these processes are independent of Ag doping. The peak associated with the crystallization of amorphous TiO_2 to anatase phase was observed at about 217 °C. The shift of the peak towards higher temperatures with respect to its position in undoped TiO_2 could be associated to the Ag doping. In contrast to the undoped TiO_2 sample, where the DSC peak corresponds anatase–rutile transformation appeared at 437 °C, the DSC curve of the Ag–TiO_2 sample prepared with 0.1698 g of $AgNO_3$ revealed this peak at about 461 °C. The peak associated with the anatase–rutile transformation shifted towards higher temperature with the increase of the used $AgNO_3$ amount in the synthesis process. The peak shifted up to 469 °C and 491 °C for the samples synthesized using 0.2831 g and 0.4247 g of $AgNO_3$, respectively. It is evident that the thermal stability of the anatase phase increases with the increase Ag doping level of the TiO_2 particles. It must be noted that our observations are in contradiction to the previously reported results of Chao et al. [38] where the anatase–rutile transformation for silver doped titania was reported to occur at lower temperatures.

In the Fig. 13, the DSC curves of the Ag–TiO_2 composite particles annealed at 300 °C in nitrogen atmosphere for 4 h are shown. From the DSC curves, we can observe an endothermic peak at about 98 °C for all the three samples, which corresponds to the dehydration process. The peak associated with the crystallization process of titania was observed at about 171 °C for the sample prepared without Ag, at about 166 °C for the sample prepared with 0.1698 g of $AgNO_3$ and at about 141 °C for the sample prepared with 0.4247 g of $AgNO_3$; which suggests that a thermal treatment at 300 °C in nitrogen atmosphere for 4 h was enough to complete the crystallization process. In addiction, the shift of the peak towards lower temperatures with respect to its position for undoped TiO_2 could be associated to the Ag doping and nitrogen atmosphere. Also, we can see a peak of anatase–rutile transformation at about 423 °C in the DSC curve of the undoped TiO_2 sample annealed at 300 °C in nitrogen atmosphere, in contrast to the DSC curve of the undoped TiO_2 sample where it appeared at about 437 °C. Similarly, the peak associated with the anatase–rutile transformation shifted towards lowers temperatures for the TiO_2 samples prepared with 0.1698 g and 0.4247 g of $AgNO_3$ and annealed at 300 °C under nitrogen in comparison with the un-annealed samples and the samples annealed in air. Therefore, the thermal stability of the anatase phase decreases when the samples are treated in nitrogen atmosphere.

4. Conclusions

TiO_2 nanoparticles doped with different Ag contents were synthesized through a modified sol–gel technique using titanium tetraisopropoxide and silver nitrate as precursors in a 2-propanol solution. Incorporation of silver in the TiO_2 particles occurs during the thermal treatment of the composite gel material through decomposition of $AgNO_3$. The XRD results indicate that when the samples are treated in air, the silver incorporates as silver oxide, while on thermal treatment in nitrogen ambient it incorporates as metallic silver. The Ag doping increases the thermal stability of the TiO_2 particles when annealed in air, enhancing the crystallization process, and inhibiting the normal anatase–rutile phase transition. It is predicted that the anatase–rutile phase transition starts from the centre of the nanoparticles, which extends to the

particle surface on prolonged thermal treatment at high temperatures. On the other hand, for the Ag–TiO_2 composite particles annealed in N_2 atmosphere, the transformation from anatase to rutile starts at temperatures below 450 °C, due to the presence metallic silver nanoparticles. Even on annealing above 600 °C, a complete anatase–rutile phase transformation does not occur as in the case of the samples annealed in air. Therefore, the thermal stability of the anatase phase depends strongly both on the Ag doping and the annealing ambient.

Acknowledgements

The work was partially supported by CONACyT, Mexico (Grant # 46269) and VIEP-BUAP (Grant # 93/EXC/2008-1), Puebla.

References

[1] K.I. Hadjiivanov, D.G. Klissurski, Chem. Soc. Rev. 25 (1996) 61.
[2] P. Forzatti, Catal. Today 62 (2000) 51.
[3] Z. Ma, Y. Yue, X. Deng, Z. Gao, J. Mol. Catal. A 178 (2002) 97.
[4] C.A. Linkous, G.J. Carter, D.B. Locuson, A.J. Ouellette, D.K. Slattery, L.A. Smitha, Environ. Sci. Technol. 34 (2000) 4754.
[5] J.K. Yang, A.P. Davis, Environ. Sci. Technol. 34 (2000) 3796.
[6] K.J. Buechler, R.D. Noble, C.A. Koval, W.A. Jacoby, Ind. Eng. Chem. Res. 38 (1999) 892.
[7] A. Maldoti, A. Molinari, R. Amadeni, Chem. Rev. 102 (2002) 3811.
[8] M. Anpo, M. Takeuchi, J. Catal. 216 (2003) 505.
[9] A. Fujishima, T.N. Rao, D.A. Tryk, J. Photochem. Photobiol. C: Photochem. Rev. 1 (2000) 1.
[10] I. Hayakawa, Y. Iwamoto, K. Kikuta, S. Hirano, Sens. Actuators, B: Chem. 62 (2000) 55.
[11] Y. Zhu, Anal. Chem. 74 (2002) 120.
[12] U. Bach, D. Lupo, P. Comte, J.A. Moser, F. Weissortel, J. Salbeck, H. Spreitzer, M. Gratzel, Nature 395 (1998) 583.
[13] M. Gratzel, Nature 414 (2001) 338.
[14] M. Adachi, J. Am. Chem. Soc. 126 (2004) 14943.
[15] S. Zhang, L.M. Peng, Q. Chen, G.H. Du, G. Dawson, W.Z. Zhou, Phys. Rev. Lett. 91 (2003) 256103.
[16] K. Mier, M. Gratzel, Chem. Phys. Chem. 3 (2002) 371.
[17] T. Paunesku, T. Rajh, G. Wiederrecht, J. Master, S. Vogt, N. Stojicevic, M. Protic, B. Lai, J. Oryhon, M. Thurnauer, G. Woloschak, Nat. Mater. 2 (2003) 343.
[18] W. Wang, B. Gu, L. Liang, W.A. Hamilton, D.J. Wesolowski, J. Phys. Chem. B 108 (2004) 39.
[19] B. Ohtani, Y. Ogawa, S. Nishimoto, J. Phys. Chem. B 101 (1997) 3746.
[20] B. Ohtani, S. Zhang, S. Nishimoto, T. Kagiya, J. Photochem. Photobiol. A: Chem. 64 (1992) 223.
[21] K. Tanaka, M.F.V. Capule, T. Hisanaga, Chem. Phys. Lett. 187 (1991) 73.
[22] M. Fernández-Garcia, A. Martinez Arias, J.C. Hanson, J.A. Rodriguez, Chem. Rev. 104 (2004) 4063.
[23] H. Tomaszewski, K. Eufinger, H. Poelmen, D. Poelman, R. Gryse, P.F. Smet, G.B. Marin, Int. J. Photoenergy 2007 (2007) 5p. (Article ID95213).
[24] F. Boccuzzi, A. Chiorino, S. Tsubota, M. Haruta, J. Phys. Chem. 100 (1996) 3625.
[25] Z. Zhang, C.C. Wang, R. Zakaria, J.Y. Ying, J. Phys. Chem. B 102 (1998) 10871.
[26] H. Kominami, S. Muratami, J. Kato, Y. Kera, B. Ohtani, J. Phys. Chem. B 106 (2002) 10501.
[27] M.A.T. Izmajlowicz, A.J. Flewitt, W.I. Milne, N.A. Morrison, J. Appl. Phys. 94 (2003) 7535.
[28] M. Epifani, C. Giannini, L. Tapfer, L. Vasanelli, J. Am. Ceram. Soc. 83 (2000) 2385.
[29] N. Perkas, V.G. Pol, S.V. Pol, A. Gedanken, Cryst. Growth Des. 6 (2006) 293.
[30] B.D. Stojanovic, Z.V. Marinkovic, G.O. Brankovic, E. Fidancevska, J. Therm. Anal. Calorim. 60 (2000) 595.
[31] P.I. Gouma, M.J. Mills, J. Am. Ceram. Soc. 84 (2001) 619.
[32] O.K. Varghese, D. Gong, M. Paulose, C.A. Grimes, E.C. Dickey, J. Mater. Res. 18 (2003) 156.
[33] M. Fernandez-Garcia, X. Wang, C. Belver, J.C. Hanson, J.A. Rodriguez, J. Phys. Chem. C 111 (2007) 674.
[34] A.G. Tompsett, A.G. Bowmaker, P.R. Gooney, B.J. Metson, A.K. Rodgers, M.J. Seakins, J. Raman Spectrosc. 26 (1995) 57.
[35] T. Ohsaka, F. Izumi, Y. Fujiki, J. Raman Spectrosc. 7 (1978) 321.
[36] S.P.S. Porto, P.A. Fleury, T.C. Damen, Phys. Rev. 154 (1967) 522.
[37] C. Xie, Z. Xu, Q.J. Yang, BY. Xue, Y.G. D, J.H. Zhang, Mater. Sci. Eng. B 112 (2004) 34.
[38] H.E. Chao, Y.U. Yun, H.U. Xiangfang, A. Larbot, J. Eur. Ceram. Soc. 23 (2003) 1457.